Received: Added at production | Revised: Added at production | Accepted: Added at production

DOI: xxx/xxxx

ARTICLE TYPE

# Predicting Short-term Mobile Internet Traffic from Internet Activity using Recurrent Neural Networks

Guto Leoni Santos*[1] | Pierangelo Rosati[2] | Theo Lynn[2] | Judith Kelner[1] | Djamel Sadok[1] | Patricia Takako Endo[3]

[1]Centro de Informática, Universidade Federal de Pernambuco, Pernambuco, Brazil
[2]Business School, Dublin City University, Dublin, Ireland
[3]Universidade de Pernambuco, Pernambuco, Brazil

**Correspondence**
*Guto Leoni Santos, Centro de Informática, Universidade Federal de Pernambuco, Pernambuco, Brazil. Email: gls4@cin.ufpe.br

**Summary**

Mobile network traffic prediction is an important input into network capacity planning and optimization. Existing approaches may lack the speed and computational complexity to account for bursting, non-linear patterns or other important correlations in time series mobile network data. We compare the performance of two deep learning (DL) architectures, Long Short-Term Memory (LSTM) and Gated Recurrent Unit (GRU), and two conventional machine learning (ML) architectures - Random Forest and Decision Tree - for predicting mobile Internet traffic using two months of Telecom Italia data for Milan. K-Means clustering was used *a priori* to group cells based on Internet activity and the Grid Search method was used to identify the best configurations for each model. The predictive quality of the models was evaluated using root mean squared error and mean absolute error. Both DL algorithms were effective in modeling Internet activity and seasonality, both within days and across two months. We find variations in performance across clusters within the city. Overall, the DL models outperformed the conventional ML models and the LSTM outperformed the GRU in our experiments.

**KEYWORDS:**
Deep Learning, Mobile Networking, Network Management, Network Optimization, Internet Traffic Prediction, LSTM, GRU

## 1 | INTRODUCTION

At the beginning of 2020, it was estimated that 67% of the global population (5.2bn people) subscribed to mobile services [1]. According to industry forecasts, we are about to enter into a period of unprecedented mobile data growth driven by the Internet of Things (IoT). According to Cisco [2], by 2023, machine-to-machine (M2M) connections that support a broad range of IoT applications will represent about 50% (14.7 billion) of total global devices and connections. By that time, 45% of all networked devices will be mobile-connected. The combination of this influx of new mobile-connected devices, faster broadband speeds, greater video consumption, and the capabilities of 5G networks is dramatically increasing mobile data traffic. The nature and scale of this growth poses significant challenges to mobile network providers including the management of complexity, scalability, Quality of Service (QoS), Quality of Experience (QoE), and privacy [3]. Constrained budgets and intense competition exacerbate these challenges.

This massive surge in demand for mobile broadband requires solutions that satisfy QoS and QoE requirements with minimum service delay and within budget constraints. Capacity planning is the process of adjusting the capacity across the network in response to changing or predicted demands [4]. Mobile network traffic modeling and prediction is an important input into multiple capacity planning tasks including network design, performance evaluation, control, and network optimization [5, 6]. Network traffic is a time series with non-linear and chaotic characteristics and is correlated over both long and short time frames [6]. There is a well-established literature that focuses on trends, seasonality and anomaly prediction to guide mobile network investments and optimization, both at the network-level and the cell-level [5, 7, 8]. Much of the existing research focuses on traffic prediction across the network that, while presenting good forecast results, may have unacceptable training and turnaround times, lack computational complexity, and consequently may not account for characteristics such as bursting, non-linear patterns or other important correlations [6, 9].

Addressing this shortcoming requires moving from coarse-grained to fine-grained prediction and the adoption of novel techniques that can accommodate high-dimensionality and provide a satisfactory solution quickly. In the last decade, we have seen a number of applications that can benefit from short-term or fine mobile network traffic prediction including opportunistic scheduling [10], multimedia optimization [11], and energy efficiency [12]. More recently, the emergence and combination of deep learning (DL) techniques and new data sources is presenting promising results in mobile traffic prediction [6, 13, 14].

This paper compares the performance of two recurrent neural networks (RNNs), Long Short-Term Memory (LSTM) and Gated Recurrent Unit (GRU), against two traditional machine learning (ML) techniques, Random Forest and Decision Tree, for predicting mobile Internet traffic. In this paper, the terms Internet activity and Internet traffic are used interchangeably. Our main contribution is the evaluation of a methodology to create clusters of cells based on statistical traffic measurements. First, cells with similar traffic patterns are grouped together, and then prediction models are created to forecast the average traffic for each cluster, since the cells of a given cluster have a similar pattern. By using this methodology, we can reduce the number of models, which improves efficiency and, as a result, reduces the computational and economic cost and complexity associated with training thousands of models.

Using two months (62 days) of spatio-temporal log data from Telecom Italia for the metropolitan area of Milan, we select 12 clusters each with its own time series. We find the best configuration of each model using the Grid Search method [15] and use root mean squared error (RMSE) and mean absolute error (MAE) to evaluate the performance of the models. Based on the results, we can state that the models satisfactorily learned the pattern of Internet activity and seasonality, both within days and across the two months. We find variations in performances based on geographic clusters within the city. Overall the LSTM performs better than the GRU in most cases. We also compare the mean absolute error (MAE) results for our models with extant research using similar data [16] and find both of our DL models significantly outperform previous work based on Random Forest and Decision Tree models.

The rest of this paper is structured as follows. In Section 2, we provide an overview of RNNs and clustering algorithms. Section 3 presents selected related research. Section 4 details the mobile Internet traffic dataset and data pre-processing, the configuration of the LSTM and GRU models, and the metrics used to evaluate model performance. Section 5 presents and discusses our results and analysis. We conclude this article with a brief summary of the main contributions of the article and propose future directions for research in Section 6.

## 2 | BACKGROUND

### 2.1 | Deep Learning Neural Networks

In the last five years, deep neural networks, 'deep learning', have increased in prominence in research and practice. DL is a sub-branch of ML that, at a high level, "enables an algorithm to make predictions, classifications or decisions based on data, without being explicitly programmed" [17]. DL addresses the limitations of single-layer neural networks by using multiple layers to transform their input into higher-dimensional representations and then into the output. The emergence of DL is largely driven by increased computational power through heterogeneous processors such as GPUs, the availability of large datasets for training, and advances in optimization algorithms [18].

In contrast to traditional ML and neural networks, DL can cater for high dimensionality in data thus enabling DL networks to model highly complex non-linear relationships between variables [18]. As such, it is particularly suitable to the mobile and wireless networking domain which is characterized by massive volumes of high velocity unlabeled heterogeneous data [17]. In addition, DL can significantly reduce operational and capital expenditure by reducing or eliminate the time and effort required

by valuable and scarce human resources in feature extraction, and reduce computational and memory requirements through multi-task learning [17]. However, DL is not without its limitations. It hides its internal logic to the user thereby sacrificing accuracy for interpretability with practical and ethical consequences [19]. Other limitations include vulnerabilities to adversarial and privacy attacks [20], computational demands unsuitable to small-form computing in edge networks, and the time taken to find optimal configurations, particularly for highly-parameterised data and multi-step network prediction [5, 17].

Common DL architectures include Multi-layer Perceptron (MLP), Restricted Boltzmann Machines (RBM), auto-encoded (AE), convolutional neural networks (CNNs), and recurrent neural networks (RNNs) [17]. These can be differentiated by the data structures that they target, and their respective tuning parameters [18]. For example, MLP targets feature vectors of fixed length and are tuned by the activation function setting and the number of layers and units [18]. In contrast, CNNs target high-dimensional data with local dependencies and are tuned by the number and width of convolutional kernels or filters [18]. Because both MLP and CNN assume that all inputs are independent of each other, they are not suited to modeling sequential data, where sequential correlations exist between samples. RNNs specifically target sequential data, like time series data flows from mobile networks. As such, we focus on the use of RNNs in this paper.

## 2.2 | Recurrent Neural Networks

### 2.2.1 | LSTM

As discussed earlier, traditional ML, MLPs and CNNs, typically target input vectors with fixed dimensions. The formalization for sequential data is fundamentally different and thus MLP and CNN are not suitable for time series data. RNN architectures were specifically designed to model sequential data by producing output via recurrent connections (cells) between hidden units [17]. These recurrent connections are the *memory* that stores the previous data allowing RNNs to learn the temporal dynamicity of the sequential data [21]. In RNNs, the output of the current timestamp is influenced by the output of the previous timestamps, which is critical when the sequence of events or data is important to determine the outcome of a problem. Despite being designed to model sequential data, early RNNs suffer from long time dependencies resulting from both vanishing and exploding gradient problems [22] that negatively impacted training using the Back-Propagation Through Time (BPTT) algorithm. To overcome this limitation, a variation of traditional RNNs was proposed, Long Short-Term Memory (LSTM), which introduces the concept of gates to mitigate gradient problems [21, 23, 24]. Figure 1 presents the basic schema of an LSTM unit.

The unit takes as input three values: the input of the current time step ($x_t$), the output from a previous LTSM unit ($h_{t-1}$), and the "memory" of the previous unit ($C_{t-1}$). The output of the LSTM unit are two values: the output and the memory of the current unit, $h_t$ and $C_t$, respectively.

The LSTM unit state updates through specific gate operations: write (input gate), read (output gate), or reset (forget gate). These operations consist of component-wise multiplications and apply different functions in the input data.

Initially, the input data, the output from previous LSTM unit, and a bias are the input for a simple one layer neural network where the activation function is sigmoid. This operation is detailed in Equation 1.

$$f_t = \sigma_f(W_{xf}x_t + W_{hf}h_{t-1} + W_{cf}C_{t-1} + b_f) \tag{1}$$

where $W_{xf}$, $W_{hf}$, and $W_{cf}$ are, respectively, the weight matrices of the forget gate for the input $x$, hidden state $h$, and the unit state $c$. $f_t$ can be defined as a "forget valve", and its output vector will be applied to the old memory, $C_{t-1}$ by element-wise multiplication, as illustrated in Figure 1.

The same inputs of $f_t$ are also passed to a second neural network with one layer but with different weight matrices:

$$i_t = \sigma_i(W_{xi}x_t + W_{hi}h_{t-1} + W_{ci}C_{t-1} + b_i) \tag{2}$$

where $i_t$ controls how much the old memory will influence the new memory of the LSTM unit. However, the new memory is generated by another neural network with one layer but a hyperbolic tangent as the activation function:

$$g_t = tanh(W_{xc}x_t + W_{hc}h_{t-1} + b_c) \tag{3}$$

Then, $i_t$ and $g_t$ are element-wise multiplied and summed to the old memory to compose the new unit memory, $C_t$, as shown in Equation 4. $C_t$ is one of the output values of the LSTM unit, as shown in Figure 1.

$$C_t = f_t c_{t-1} + i_t g_t \tag{4}$$

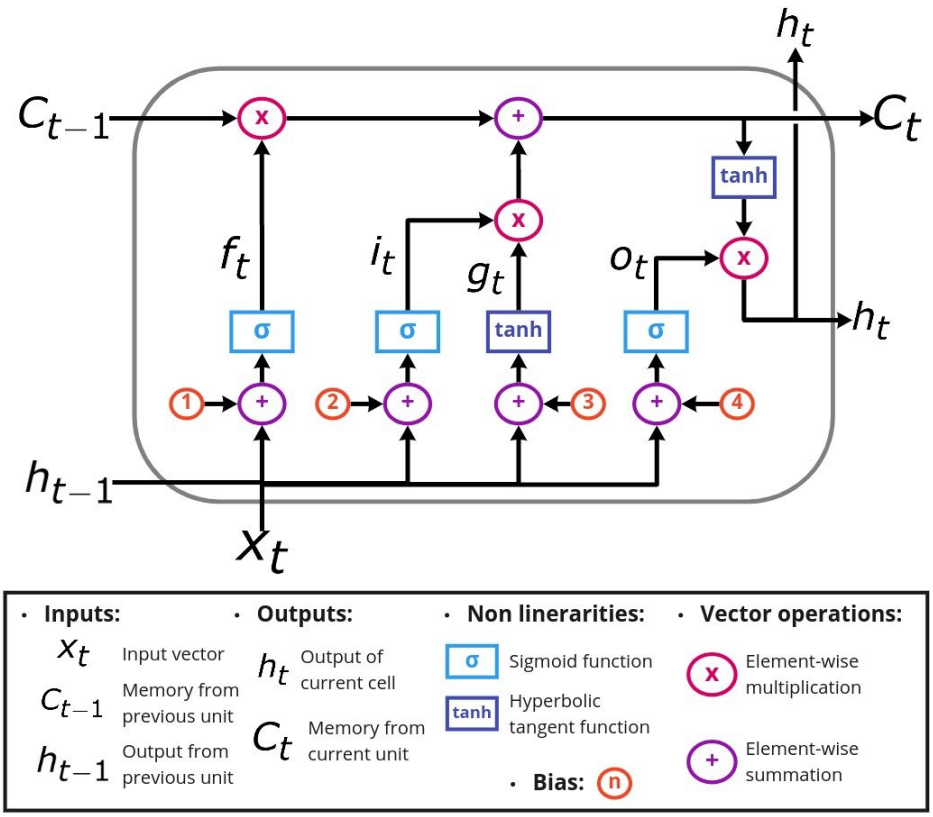


**Figure 1** Example of a LSTM unit (adapted from [25]).

Finally, the unit output, $h_t$, is impacted by the new memory, the previous output $h_{t-1}$, and the input $X_t$. $o_t$ is a neural network similar to $i_t$ and $f_t$, with one layer and sigmoid as activation function. It receives as input $X_t$ and $h_{t-1}$. As shown in Equation 5, the tangent hyperbolic activation function is applied in $C_t$ and then element-wise multiplied by $o_t$. $h_t$ controls how much new memory should output to the next LSTM unit.

$$h_t = o_t tanh(c_t) \tag{5}$$

While LSTM addresses gradient problems, critics have noted that the LSTM architecture is *ad hoc*, has a substantial number of components whose purpose is not immediately apparent, and that it is characterized by long training times [23, 26].

Given its ability to model time series data and predictive capacity, we use LSTM in this study.

### 2.2.2 | GRU

GRU is a variation of LSTM which only uses two gates, an update gate and a reset gate. Indeed the update gate in a GRU replaces the input and forget gates used in LSTM and decides what input data will be kept [27]. Furthermore and unlike LSTM, GRU exposes its memory content at each step balancing between the previous and new memory content [28].

The GRU activation, $h_t^j$, is represented in Equation 6. Considering the input data as a time series, at the timestamp $t$, $h_t^j$ is the linear interpolation between the previous unit data ($h_{t-1}^j$) and the current data ($\tilde{h}_t^j$).

$$h_t^j = (1 - z_t^j)h_{t-1}^j + z_t^j \tilde{h}_t^j \tag{6}$$

where $z_t^j$ is the output gate, and defines what should be forgotten and what should be kept in the GRU unit. The output gate is defined in Equation 7 [28]:

$$z_t^j = \sigma(W_z x_t + U_z h_{t-1}) \tag{7}$$

where the current and previous weight matrices are $W_z$ and $U_z$, respectively. In a simplified way, this procedure taking a linear sum between the previous hidden states $h_{t-1}$ and the current input $x_t$ and applies the sigmoid function ($\sigma$).

The new memory unit is calculated as described in Equation 8:

$$\tilde{h}_t = than(W x_t + r_t \odot U h_{t-1}) \tag{8}$$

where $\odot$ is the element-wise multiplication, $r_t$ refers to reset gate, and its output can be calculated as defined in Equation 9:

$$r_t = \sigma(W_r x_t + U_r h_{t-1}) \tag{9}$$

Research suggests that GRUs are easier to generalize with faster training times while achieving comparable performance outcomes [23, 28, 29, 30]. As such, we also propose a GRU for comparison against LSTM and ML models in this study.

## 2.3 | Clustering

Clustering is an unsupervised ML technique that breaks down a dataset into disjointed groups (clusters) of observation with similar characteristics [31]. There is a variety of clustering techniques [32]; K-Means clustering is the most widely used technique. The K-Means algorithm is a partitioning method which groups unlabeled data into a predefined $k$ number of clusters based on the Euclidean distance between different data vectors [33].

The K-Means algorithm starts by randomly selecting a $k$ number of centroids; it then calculates the distance between a data vector and each centroid and assigns the vector to the cluster with the closest centroid as outlined in Equation 10 [33].

$$S_i^{(t)} = \left\{ x_p : \left\| x_p - \mu_i^{(t)} \right\|^2 \leq \left\| x_p - \mu_j^{(t)} \right\|^2 \ \forall j, 1 \leq j \leq k \right\} \tag{10}$$

where $S$ is the distance between the element and the centroid; $i$ is the cluster number; $t$ is the number of iterations; $x_p$ is point value; $\mu^{(t)}$ is the value of centroid; and $j$ is the measure of dissimilarity.

Every time a new data vector is assigned to a cluster, the K-Means algorithm calculates a new centroid based on the average of distances of all data points in each cluster as presented in Equation 11. This iterative process is completed when all data vectors have been allocated to different clusters and the ultimate centroids are identified.

$$\mu_i^{(t+1)} = \frac{1}{|S_i^{(t)}|} \sum_{x_j \in S_i^{(t)}} x_j \tag{11}$$

We are seeking to predict mobile Internet traffic across a city comprising multiple cells. Traffic behavior may vary across different cells and the behavior of one cell is not necessarily similar to its neighboring cell. As such, we propose a methodology based on cell clustering to predict the Internet traffic using K-means clustering.

# 3 | RELATED WORKS

Predicting traffic for the next day, hour, or even the next minute can be used to optimize the available system resources, for example by reducing the energy consumption, applying opportunistic scheduling, or preventing problems in the infrastructure [8].

Zhang et al. [34] proposed a CNN model that was able to capture the spatial dependency and two temporal dependencies, closeness and period. Prediction matched the ground truth trend well, and the peaks of both incoming and outgoing traffic was effectively captured and predicted compared to three existing algorithms - Historical Average value, Auto-Regressive Integrated Moving Average (ARIMA) and LSTM. Huang et al. [10] propose a multi-task learning architecture with three different types of DL models including LSTM, three-dimensional CNN, and a combination of CNN and RNN (CNN-RNN) to model spatial and temporal aspects of the traffic. They also compare the performance against ARIMA and non-DL methods. The CNN-RNN model was found to be reliable for all tasks with 70 to 80% forecasting accuracy. Chen et al. [16] propose a two-phase framework to dynamically find optimal Remote Radio Head (RRH) clustering and Baseband Unit (BBU) mapping schemes under different contexts. A multivariate LSTM was used to learn the temporal dependency and spatial correlation among base station traffic patterns, and make accurate traffic forecasts for future time periods. The prediction output was used to create RRH clusters and map them to BBU pools to maximize the average BBU capacity utility and minimize the overall deployment cost. Results suggested that the proposed method increased the average capacity utility and reduced the overall deployment cost outperforms

baseline methods i.e. Distance-Constrained Complementarity-Aware (DCCA) ARIMA, DCCA Windowed Artificial Neural Networks (DCCA-WANN), and multivariate distance-constrained LSTM. Wang et al. [35] propose a hybrid DL model for spatio-temporal prediction comprising of an AE-based model for spatial modeling, and LSTM for temporal modeling. Results suggest that the proposed hybrid model significantly improves prediction accuracy compared to ARIMA and Support Vector Regression (SVR). In Alawe et al. [36], an LSTM and a deep neural network model were compared for predicting traffic load on a 5G network to inform a scalability mechanism. Performance was evaluated using simulation and suggests that the forecast-based scalability mechanism outperformed threshold-based solutions.

Unlike the other Telecom Italia studies cited above, Zhang and Patras [37] focus on reliable *long-term* mobile data traffic forecasting. They propose an ensemble system that leverages convolutional LSTM and 3D-ConvNets structures to model long-term trends and short-term variations of the mobile traffic volume, respectively. Results suggest that the proposed system provided highly accurate long term (10-hour long) traffic predictions, while operating with short observation intervals (2 hours), irrespective of the time of day. The ensemble system outperformed baseline methods including Holt Winters (HW), ARIMA, MLP, and Support Vector Machine (SVM).

Wang et al. [35] propose a novel decomposition of in-cell and inter-cell urban data traffic, and apply a graph-based neural network (GNN) using LSTM to accurately predict mobile traffic. They compare their proposed GNN with a number of baseline methods including NAIVE, ARIMA, LSTM, HW, and variations of their GNN. Results suggest that the proposed DL variant of their GNN consistently and significantly outperformed all the baselines in both MAE and Mean Absolute Relative Error (MARE). Feng et al. [38] propose an LSTM-based end-to-end model (DeepTP) to forecast traffic demands from spatial-dependent and long-period cellular traffic. DeepTP outperforms ARIMA, SVR, and GRU (although to a lesser extent) based on MRSE. While outperforming other models, DeepTP was much slower than other models including GRU. Qiu et al. [14] also use LSTM combined with unified multi-task learning frameworks to explore spatio-temporal correlations among base stations to improve traffic prediction. They evaluate their proposal against Online SVR, Non-parametric Regression, the Adaptive Kalman filters, and an AE approach. The proposed LSTM-approach outperforms other methods using MSE as a performance metric.

Even though a number of studies have already tried to address the challenges posed by mobile traffic prediction, our work proposes a different methodology. While other studies have clustered cells based on their geographical location, in this study we group them based on traffic similarity in order to mitigate traffic variation and therefore improve traffic prediction. In addition, we test and compare two different DL approaches and associated configurations to identify the most effective model for traffic prediction. We also compare these DL models with Random Forest and Decision Tree, which are traditional ML models used for time series forecast.

# 4 | MATERIAL AND METHODS

## 4.1 | Dataset

The metropolitan area of Milan is located in northern Italy and consists of nine different municipalities (see Figure 2). Milan is the largest metropolitan area in Italy and one of the ten most populous in the European Union [39].

In this study, we use the Telecom Italia dataset for Milan from the *Big Data Challenge* [40]. The dataset is organized into 10,000 cells (100 x 100) comprising over 10 million user activity logs, each related to a particular cell. The dataset has log data for two months (62 days) from 1 November 2013 to 1 January 2014 [41]. Although this dataset was collected between 2013 and 2014, it still proves to be quite valuable for researchers exploring mobile traffic prediction and it has been used in a number of recently published articles (see, for example, [42, 43, 44]). The Telecom Italia dataset adopted in this study in fact is one of the few telecommunication datasets that are publicly available in contrast to the large number of datasets that are typically accessible to a restricted number of researchers under non-disclosure agreements (NDAs), or by third parties that have a contractual relationship with telecommunication providers.

The log activity is structured as Call Detail Records (CDRs) on the following activities: (i) incoming and outgoing voice calls, (ii) short message service (SMS) messages, and (iii) Internet activity. A CDR is generated every time a user starts or finishes a voice call, sends or receives an SMS, and starts or terminates an Internet session (the data is recorded if the connection takes more than 15 minutes, or more than 5 MB is transferred during the session). In this paper, we specifically focus on predicting Internet traffic.

As the dataset has periods with no Internet traffic (e.g., a few minutes at night where there are no records), we aggregate all CDRs for Internet traffic into 30-minute periods. Consequently, we have 48 records per day related to Internet traffic. We use

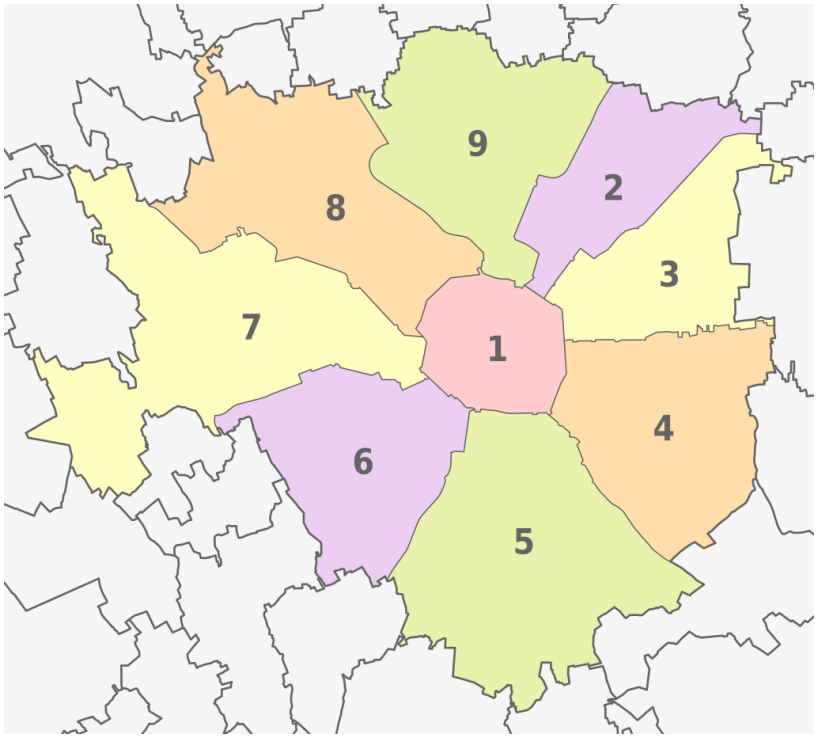


**Figure 2** The Milan Metropolitan Area.
Source: https://www.wikiwand.com/en/Municipalities_of_Milan

a sliding window strategy with a window size of four time periods thus we use the previous two hours to predict the Internet activity of the subsequent 30 minutes.

To create the training and testing datasets, the original dataset is divided in two parts: the first 80% of the time series for training and the last 20% for testing. We also normalized these datasets to the [0,1] range to facilitate the training of DL models, since their parameters are very small, close to zero.

## 4.2 | Traffic Prediction Pipeline

Analysing the traffic of the cells present in the Telecom Italia dataset, we noted that there are different traffic patterns. For example, Figures 3a and 3b show the traffic of the cells 1 and 1000, respectively. The traffic of these cells is quite different. Cell 1 has some peaks at the beginning of the time series, with the biggest peak at middle of November 2013; in December the traffic is more stable. On the other hand, Cell 1000 traffic has regular peaks across November and December. At the end of December, Cell 1000 traffic drops, this does not happen in any other period of the time series, nor in Cell 1 traffic.

The traffic of these cells reinforces the complexity and dynamism of the scenario under study; different parts of Milan present different traffic across the periods. This poses a challenge when using just one model to predict the traffic for all cells, since DL models learn the pattern from the input data. Therefore, if a DL model trained with the Telecom Italia dataset learns the pattern of Cell 1 traffic, it may present a high error to predict the traffic of the Cell 1000, due to the different patterns. On the other hand, to create a prediction model for each cell present in the dataset will result in 10,000 models, which can be complex to manage, since these models must be trained and re-trained if the traffic pattern of the cells changes.

In order to deal with these issues, we create clusters of cells based on their traffic prediction patterns. Figure 4 illustrates the pipeline used to create the cells' clusters to make the traffic prediction. Initially, we calculate the traffic of each cell present in the Telecom Italia dataset. Afterwards, we create clusters of cells based on the traffic statistics, as we will explain in Subsection 4.3. We group all cells with similar traffic patterns into a cluster. Once the clusters of cells are created, we calculate the mean traffic of all cells for each cluster, composing $N$ time series, where $N$ is the number of clusters. These time series (mean traffic of each cluster) are used to train DL models for traffic prediction. Instead of training one model for each cell, which results in a high number of models to train (e.g. for the Milan region, approximately 10,000 DL models would need to be trained and

managed), we create $N$ DL models, one for each cluster. Since the traffic for cells in a given cluster have a similar pattern, the model of the respective cluster can be used to predict traffic of the cells that compose that cluster. Cell clusters are discussed in more detail in the next subsection.

Since the DL models of each cluster are trained with the mean traffic of the respective cluster, we can use these models to predict the mean traffic for each cluster, the last step in our pipeline. To evaluate the performance of the DL models, we use RMSE and MAE as metrics as detailed later in Subsection 4.5.

## 4.3 | Clustering the Cells

The dataset is composed of traffic data for different cells for Milan. As discussed previously, we propose a methodology based on cell clustering using Internet activity as a statistical metric to propose DL models to predict Internet traffic. We calculate the total number of Internet activities considering six periods in each day, as described in Table 1[1]

**Table 1** Periods of the day.

| Period | Time (in hour) |
|---|---|
| Late Night | 00:00 - 04:00 |
| Early Morning | 04:00 - 08:00 |
| Morning | 08:00 - 12:00 |
| Afternoon | 12:00 - 16:00 |
| Evening | 16:00 - 20:00 |
| Night | 20:00 - 00:00 |

Each cell can be represented by a vector containing six values based on the average Internet activity for each period of the day. Based on these values, we create clusters of cells using the K-Means algorithm [33] which has been widely used in a number of different research domains such as document classification, recommendation systems based on user interests, classification based on user purchase behavior etc. The K-Means algorithm has many advantages compared to other clustering techniques including ease of implementation and fast convergence, even for Big Data [45].

To automatically estimate the optimal number of clusters ($k$) of cells, we applied the Elbow method. This method varies the number of clusters within a range to find the optimal $k$ based on the sum of square error [46]. We varied $k$ from one to 50 as shown in Figure 5. As the number of cluster increases, the sum of squared distance tends towards zero with the elbow of curve being the optimal value. In our case, we select $k = 12$ since it is at the end of the elbow and the beginning of the stabilization

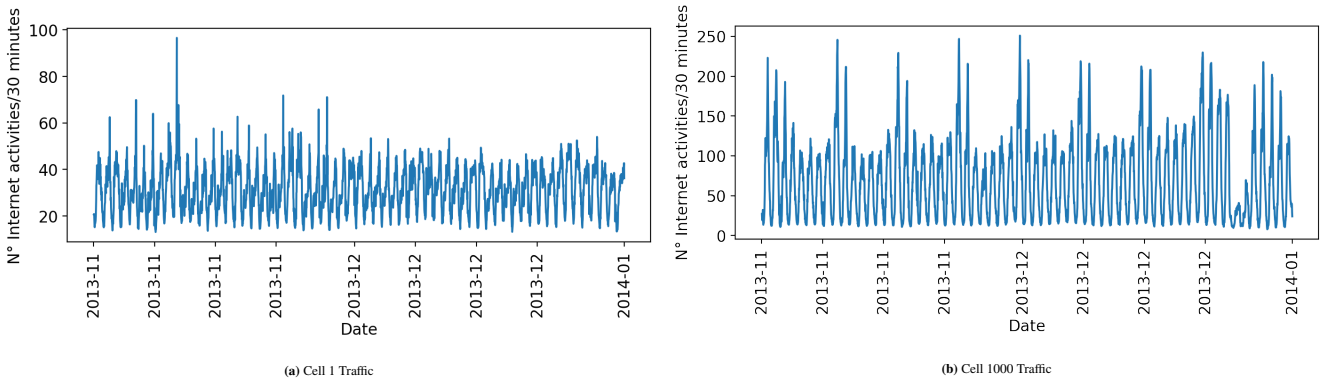


**(a)** Cell 1 Traffic

**(b)** Cell 1000 Traffic

**Figure 3** Number of Internet activities of cells 1 and 1000 in the Telecom Italia dataset.

[1] In Northern Italy, unlike other countries where lunch is 1230-1400, the working day often includes a break from 1200-1330 or 1430-1600. For the purposes of this study, we have aggregated this as a four hour block. Researchers may need to modify this for other countries.

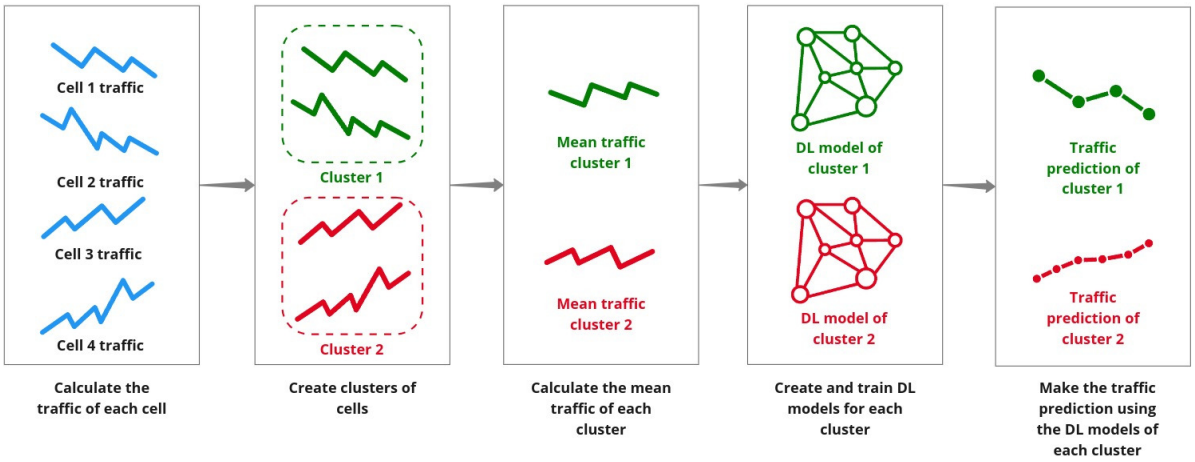


**Figure 4** Cell internet traffic prediction pipeline.

of the sum of the squared distances. Based on the results presented in Figure 5, using more than 12 clusters would only increase the complexity of the algorithm with no significant gains in terms of performance.

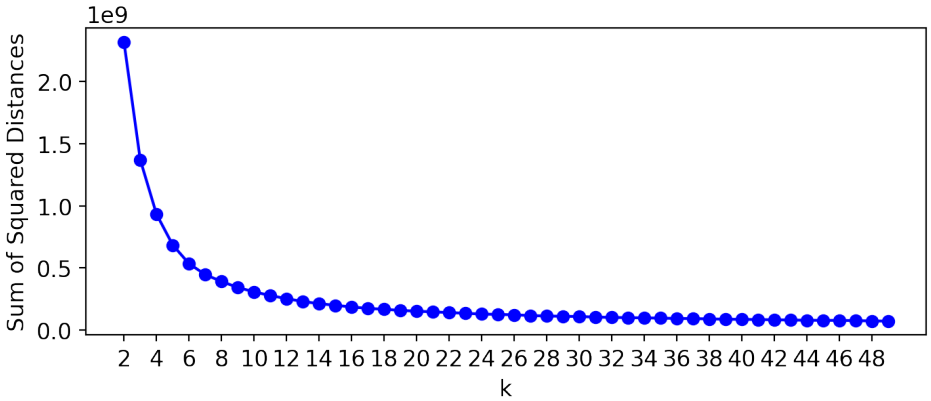


**Figure 5** Elbow method results.

The 12 clusters have a similar Internet activity pattern across different time periods within each day, regardless of the cell location. Figure 6 shows the 12 clusters overlaid on a map of the Milan Metropolitan Area. To some extent, Cluster 1 represents the external areas of Milan; Cluster 10 represents the border of the municipalities (excluding the municipality 1 in the center), while Cluster 6 is at the center of such municipalities. Other Clusters (2, 3, 4, 5, 7, 8, 9, 11 and 12) are regions within the city.

We calculate the mean Internet traffic for each of the 12 clusters using the 30-minute aggregated traffic of all cells included in each cluster divided by the number of cells of the cluster. Thus, for each cluster, we have a time series related to their mean cell's traffic. This time series is used to train and test the proposed DL models.

## 4.4 | DL Model Configuration

In this paper, we propose two different RNNs that are widely used in the DL literature for regression problems, LSTM and GRU. To find the best configuration of the models, we apply a technique called Grid Search. This technique performs an exhaustive search in a subset of the previously defined parameters and provides the near optimal parameter combination within the given range [15]. To apply the Grid Search, we vary the number of hidden layers and their units for both LSTM and GRU (see the parameters and levels in Table 2).

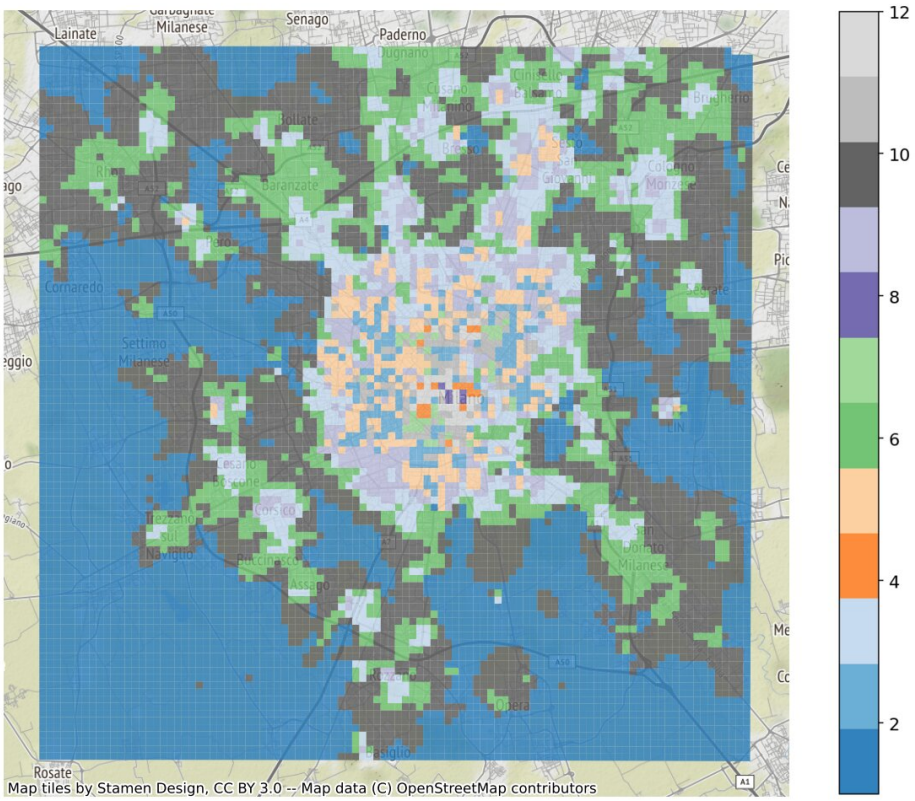


**Figure 6** Overlay of the 12 clusters on a map of the metropolitan area of Milan.

**Table 2** Grid Search parameters and levels.

| Parameters | Levels |
|---|---|
| Number of layers | 1 to 4, step 1 |
| Number of units | 50 to 150, step 50 |

The first layer of the model is a fixed recurrent layer (the same as the hidden layers) where the number of units equals the input data length. The last layer is a fully connected layer with one neuron that gives the prediction value. Table 3 shows the fixed parameters (empirically chosen) to train the DL models.

Due to the random characteristics that exist in training (e.g. initialization of weights, selection of batches etc.), we perform the experiments 30 times and calculate the average RMSE and the average MAE.

## 4.5 | Metrics for evaluating DL models

To assess the performance of the models, we use two metrics: RMSE and MAE. The RMSE metric is calculated as per Equation 12:

$$RMSE = \sqrt{\frac{1}{N}\sum_{i=1}^{N}(f_i - y_i)^2} \tag{12}$$

**Table 3** Parameters used to train the DL models.

| Parameter | Value |
|---|---|
| Activation function of recurrent layers | sigmoid |
| Activation function of last layer | hard sigmoid |
| Number of epochs | 50 |
| Optimizer | ADAM [47] |
| Learning rate | 0.001 |
| Batch size | 32 |
| Loss function | mean squared error |
| Number of runs | 30 |

where $N$ is the number of points from the traffic series, $f_i$ is the model prediction at timestamp $i$, and $y_i$ is the the real value at timestamp $i$ [48]. We use RMSE because it measures the deviation between the true value and the value predicted by the model, and is widely used in extant literature for evaluating traffic prediction models [34, 49, 50, 51].

We also used MAE to evaluate the DL models. In contrast to RMSE, MAE assigns the same weight to all errors [52]. MAE can be calculated as per Equation 13:

$$MAE = \frac{1}{N}\sum_{i=1}^{N}|f_i - y_i| \tag{13}$$

where $N$ is the length of time series, $f_i$ is the prediction, and $y_i$ is the actual value of timestamp $i$. Similar to the RMSE, MAE is widely used in the literature to evaluate traffic prediction models [53, 54, 55].

## 5 | RESULTS

We use only the RMSE metric to assess the different DL architectures performance and find the best configuration for each one. In the Subsection 5.2 we use both RMSE and MAE to compare the best configurations of DL models between them and against ML models. Figures 7 and 8 present the Grid Search RMSE results for each cluster for each of the LSTM and GRU models, respectively. For the LSTM models (Figure 7), for the majority of the clusters, the best configuration has one layer and 250 units. The only exception is Cluster 12, where the best overall average RMSE is achieved using a configuration with one layer and 150 units (LSTM-12-1L-150U) and one layer with 200 units (LSTM-12-1L-200U). Cluster 1 achieves the worth average RMSE result (0.084) while Cluster 12 achieves the best average RMSE result (0.068).

For GRU (Figure 8), the configurations with one layer present the best average RMSE, however the performance of different clusters varies based on the number of units. From Cluster 2 to Cluster 9 (GRU-2-1L-200U, GRU-3-1L-200U, GRU-4-1L-200U, GRU-5-1L-200U, GRU-6-1L-200U, GRU-7-1L-200U, GRU-8-1L-200U, and GRU-9-1L-200U), the configuration with the lowest average RMSE is one layer with 200 units. For Clusters 1 and 10, the configuration that provides the best average RMSE is one layer with 250 units (GRU-1-1L-250U and GRU-10-1L-250U). In Clusters 11 and 12, two configurations have the best average RMSE, all with only one layer. For Cluster 11, the best configurations have 150 units (GRU-11-1L-150U) and 250 (GRU-11-1L-250U) units while for Cluster 12 the best performing configuration has 150 units (GRU-12-1L-150U) and 200 units (GRU-12-1L-250U). Similar to LSTM, the clusters with the worst and best average RMSE are Cluster 1 (0.0091) and Cluster 12 (0.0045), respectively.

The complexity of the model is directly related to the number of layers and units i.e. the more layers and units, the more complex the model becomes. Model complexity has to be adjusted according to the data. Figures 7 and 8 illustrate that very complex models (those with many layers and units) resulted in poorer performance, due to model overfitting. Simpler models with less complexity also performed poorly, most likely due to model underfitting.

In general, the DL models with one hidden layer obtain better average RMSE results than models with more layers; while those with 150 units or more result in better average RMSE results. Fine-tuning the models by increasing the number of units rather than layers result in better performance. Adding hidden layers results in performance degradation.

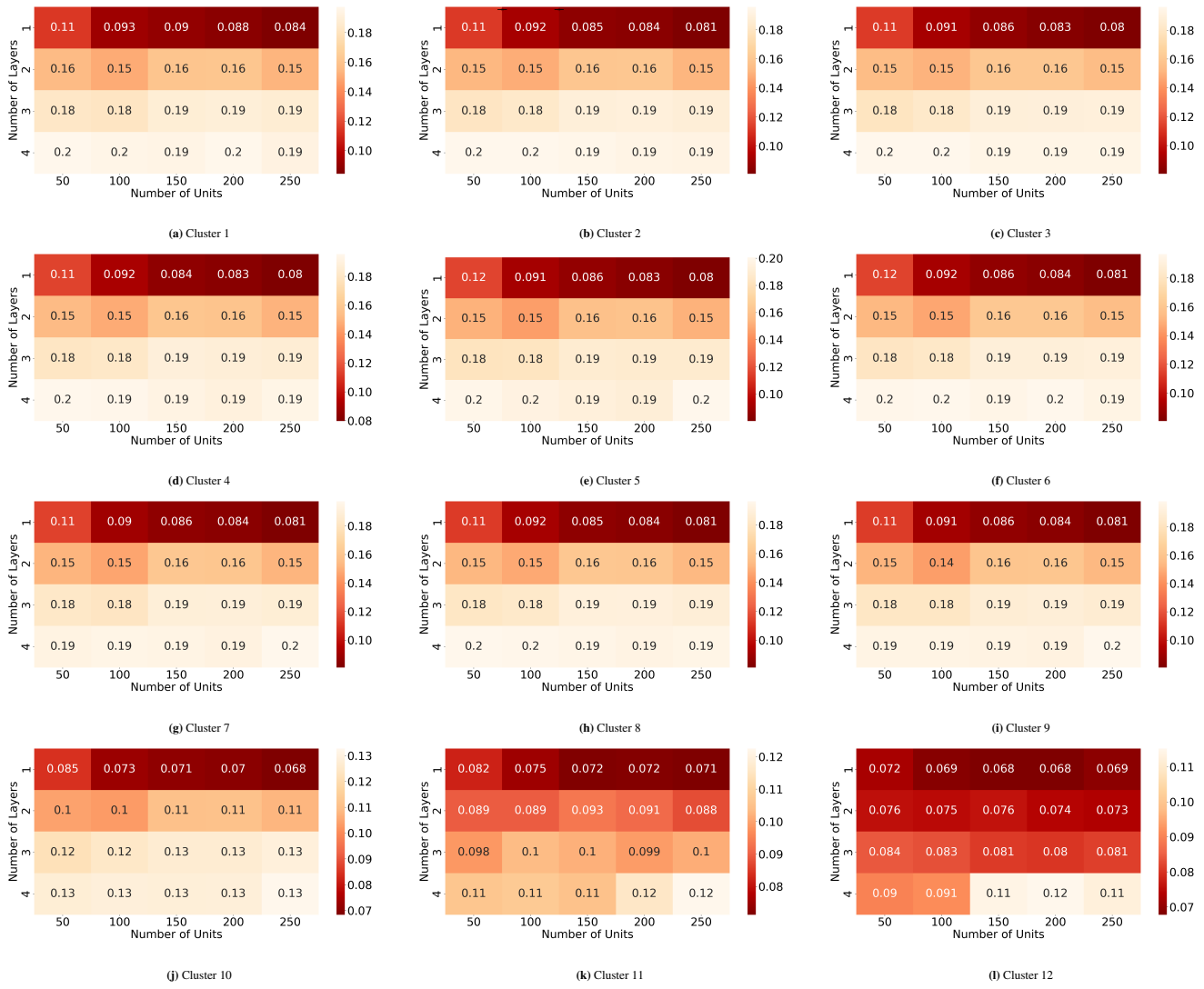


**Figure 7** Average RMSE of the LSTM model all clusters.

## 5.1 | Statistical analysis

Some configurations achieved by the Grid Search obtained very similar average RMSE. To explore this further, we use Kruskal-Wallis non-parametric analysis to compare independent samples to check whether they are similar or not, based on the mean ranks of these samples [56].

In our LSTM results, Cluster 12 (LSTM-12-1L-150U and LSTM-12-1L-200U) has two configurations with the same average RMSE. Figure 9 presents the box plot of the RMSE of these Cluster 12 configurations.

While the best Cluster 12 configurations have the same average RMSE (0.068), they have different RMSE distributions. We can note that the LSTM-12-1L-200U has a lower dispersion and a lower median than LSTM-12-1L-150U. LSTM-12-1L-200U has an outlier below the minimum RMSE value, and LSTM-12-1L-150U has an outlier above of the maximum RMSE value. This analysis suggests that LSTM-12-1L-200U is the best configuration since it has the lowest dispersion and the lowest median.

For the GRU models, Clusters 1-3 and 5-9 each had at least one statistically similar best configuration (Figure 10). For Clusters 1-3 and 5-7, the configurations with 250 units (GRU-1-1L-250, GRU-2-1L-250, GRU-3-1L-250, GRU-5-1L-250, GRU-6-1L-250 and GRU-7-1L-250) presented a higher dispersion than the configurations with 200 units (GRU-1-1L-200, GRU-2-1L-200, GRU-3-1L-200, GRU-5-1L-200, GRU-6-1L-200 and GRU-7-1L-200); GRU-1-1L-200 presented a higher median than GRU-1-1L-250. For Cluster 8, three models are statistically similar, those with one layer and 150, 200, and 250 units. Again, the configuration with 200 units presented lower dispersion and a lower median than the other configurations. Finally, both

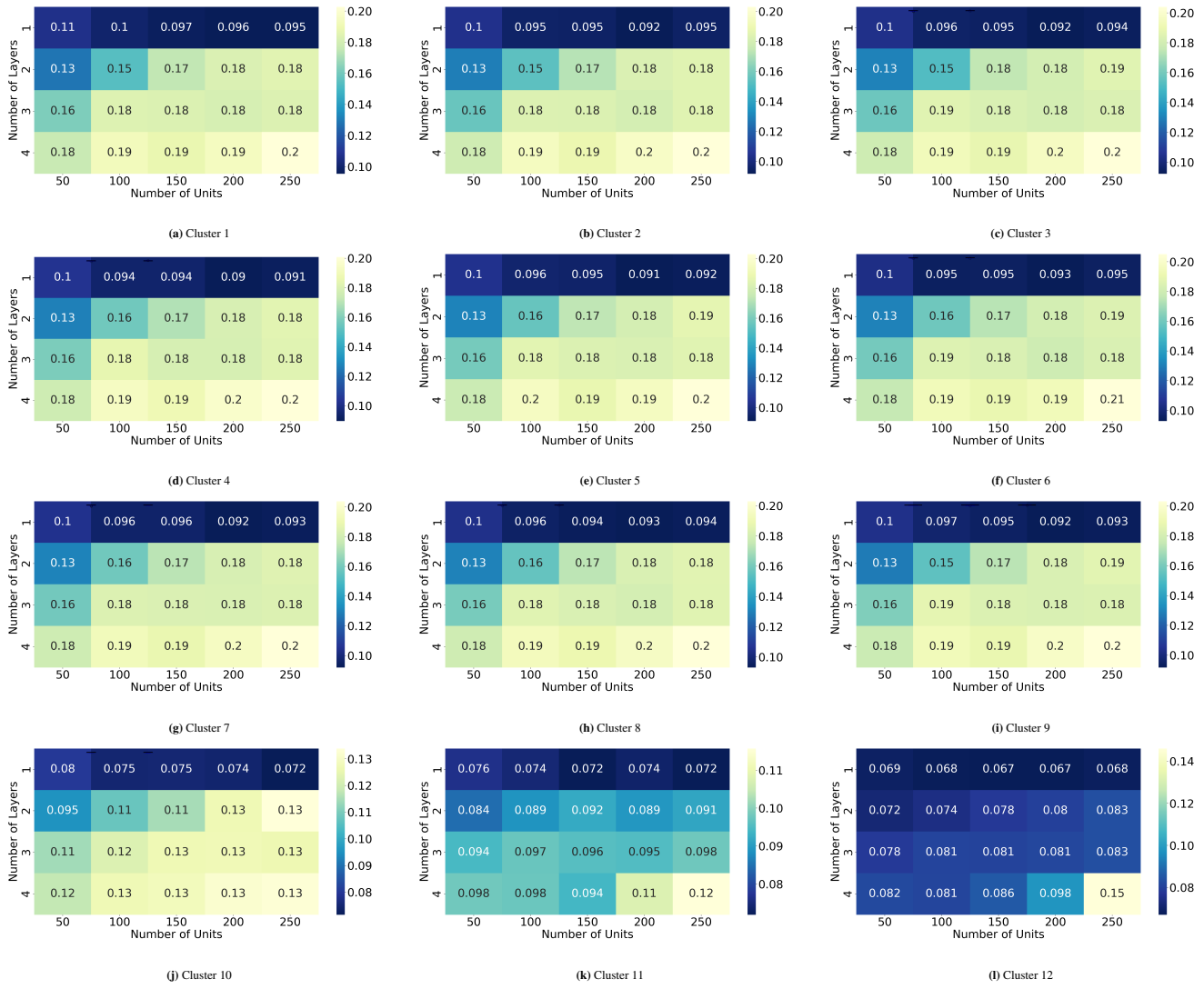


**Figure 8** Average RMSE of the GRU models for all clusters.

configurations of Cluster 9 (GRU-9-1L-200 and GRU-1-1L-250) had very similar distributions, with similar dispersion and a similar median. In general, for these clusters with statistically similar configurations, the configuration with one layer and 200 units presented a lower dispersion and lower median; this is considered the best performing configuration for the GRU models.

## 5.2 | Comparison of LSTM and GRU models.

Table 4 presents the results for the RMSE and MAE metrics, comparing the LSTM and GRU models against two traditional ML models as baseline: Random Forest and Decision Tree. For each cluster, we created the DL and ML models, then trained and evaluated with the same training and testing datasets 30 times and calculated the average RMSE and MAE.

The DL models outperform the ML models for all clusters based on the RMSE and the MAE results. For the Cluster 1, the LSTM has a reduction of 50.32% in average RMSE and a reduction of 51.99% in average MAE when compared with Random Forest. Considering the Decision Tree, the LSTM presents a reduction of 62.67% in the average RMSE and a reduction of 62.96% in the average MAE. In the Cluster 1, comparing the GRU and Random Forest, the GRU has a reduction of 43.78% in the average RMSE and 45.66% in the average MAE. In the same cluster, the GRU presents a reduction of 57.64% and 58.08%, for the average RMSE and MAE respectively, when compared with Decision Tree.

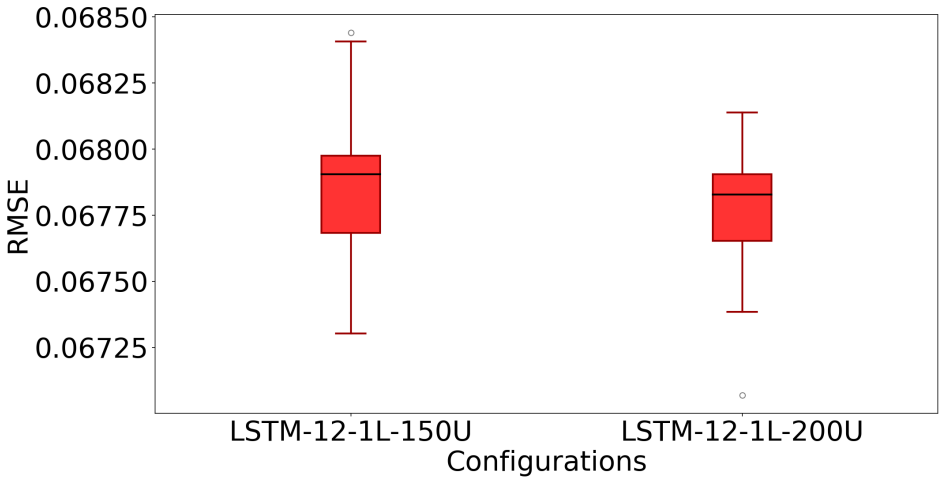


**Figure 9** Box plot of the RMSE of the best LSTM configurations for Cluster 12.

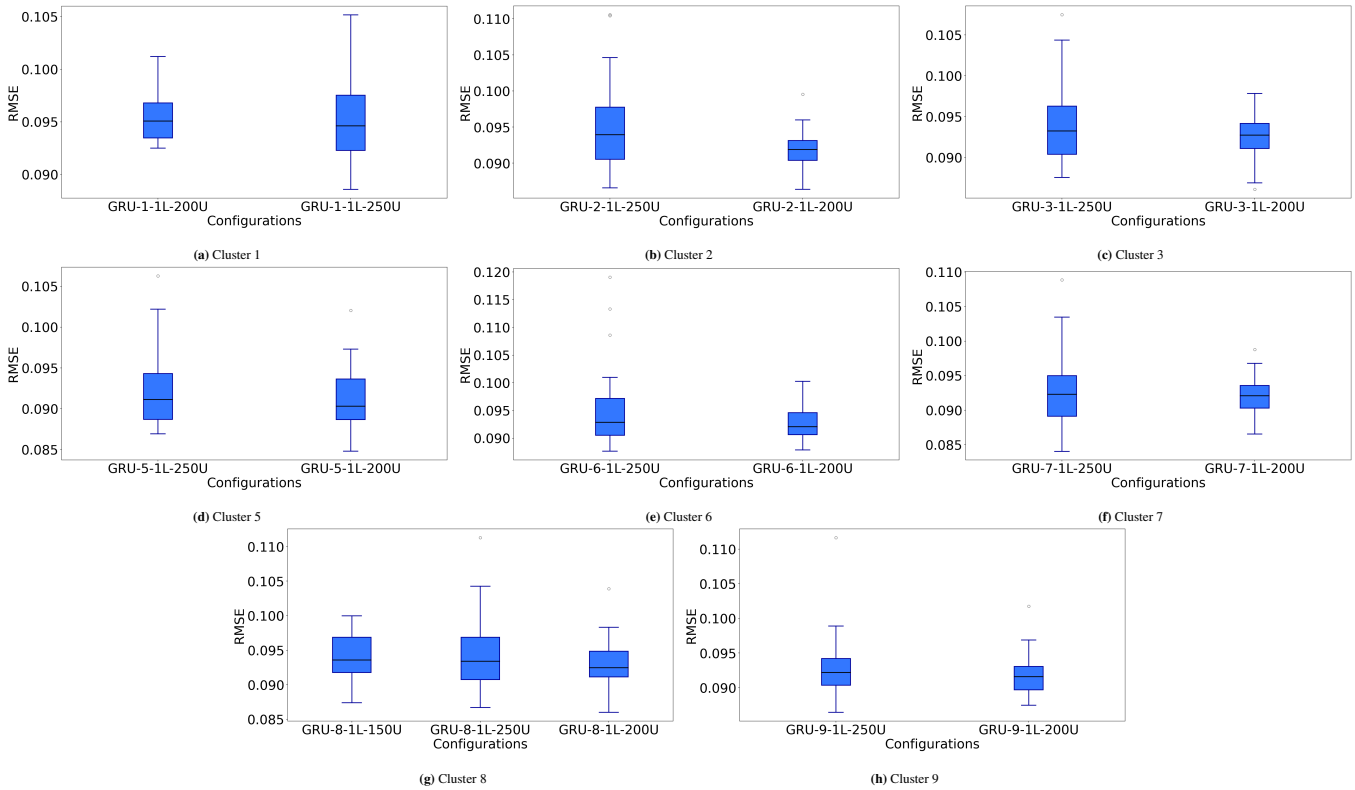


**Figure 10** Boxplot of the RMSE of the best configurations of GRU models.

The DL models are clearly superior to the conventional ML models for traffic prediction tasks; the ML models cannot achieve the same level of prediction error of DL models based on the RMSE and the MAE.

ML model results suggest that the Random Forest model outperforms the Decision Tree model for all clusters. For Cluster 1, the Random Forest model presents an average RMSE of 0.1695, while the Decision Tree model presented an average RMSE of 0.2251, a difference of 24.70%. For Cluster 1, the Random Forest and Decision Tree present an average MAE of 0.1360 and 0.1763, respectively, a difference of 29.63%.

**Table 4** Comparison of the LSTM, GRU, Random Forest, and Decision Tree models.

| Cluster | LSTM | | GRU | | Random Forest | | Decision Tree | |
|---|---|---|---|---|---|---|---|---|
| | **RMSE** | **MAE** | **RMSE** | **MAE** | **RMSE** | **MAE** | **RMSE** | **MAE** |
| 1 | 0.0842 | 0.0653 | 0.0953 | 0.0739 | 0.1695 | 0.1360 | 0.2251 | 0.1763 |
| 2 | 0.0809 | 0.0639 | 0.0917 | 0.0716 | 0.1664 | 0.1330 | 0.2200 | 0.1677 |
| 3 | 0.0803 | 0.0634 | 0.0922 | 0.0720 | 0.1645 | 0.1316 | 0.2202 | 0.1670 |
| 4 | 0.0796 | 0.0629 | 0.0896 | 0.0701 | 0.1699 | 0.1348 | 0.2052 | 0.1630 |
| 5 | 0.0800 | 0.0632 | 0.0909 | 0.0709 | 0.1602 | 0.1276 | 0.2007 | 0.1567 |
| 6 | 0.0806 | 0.0636 | 0.0928 | 0.0724 | 0.1665 | 0.1331 | 0.2198 | 0.1671 |
| 7 | 0.0807 | 0.0638 | 0.0920 | 0.0718 | 0.1675 | 0.1339 | 0.2185 | 0.1654 |
| 8 | 0.0808 | 0.0639 | 0.0929 | 0.0725 | 0.1684 | 0.1347 | 0.2208 | 0.1680 |
| 9 | 0.0805 | 0.0636 | 0.0917 | 0.0716 | 0.1680 | 0.1345 | 0.2219 | 0.1699 |
| 10 | 0.0683 | 0.0544 | 0.0715 | 0.0564 | 0.0957 | 0.0740 | 0.1084 | 0.0824 |
| 11 | 0.0712 | 0.0564 | 0.0719 | 0.0565 | 0.0842 | 0.0627 | 0.1072 | 0.0788 |
| 12 | 0.0677 | 0.0546 | 0.0671 | 0.0539 | 0.0784 | 0.0580 | 0.1035 | 0.0772 |

We compared the best configurations for the LSTM and GRU models for each cluster using the Kruskal-Wallis test. The best configurations of LSTM and GRU based on the number of layers and RNN units were selected using the lowest average RMSE values (see Figures 7 and 8). We consider 30 RMSE values obtained from experiments. For all clusters, the RMSE distributions of the LSTM and GRU models are statistically different. From Table 4, one can note that the LSTM models obtain better average RMSE and MAE results except for Cluster 12, where the GRU slightly outperforms the LSTM.

Cluster 1 presents the worst results for RMSE and MAE. LSTM presents an average RMSE of 0.0842, while the GRU presents 0.0953, a difference of 13.18%. In the MAE results for Cluster 1, the LSTM presents 0.0653, while the GRU presents 0.0739, a difference of 13.17%. In contrast, Cluster 12 has the best average RMSE, 0.0677 and 0.0671 for LSTM and GRU, respectively, with a difference of 0.89%. For the same cluster, the LSTM and GRU present an average MAE of 0.0546 and 0.0539, respectively, with a difference of 1.28%.

To help understand the difference between the performance of the models across the clusters, we visualise the actual Internet activity (green line), the LSTM model internet traffic predictions (blue line), and the GRU model internet predictions (orange line) (see Figure 11). For visualisation and sensemaking purposes, we omit the ML model predictions.

Both models learned the pattern of Internet activity data, capturing its seasonality. For Clusters 1-9, the models' predictions are slightly lower than the ground truth data in some periods, with the GRU prediction values lower than the LSTM predictions, consistent with the GRU models' higher average RMSE and MAE results. For Clusters 10-12, the predictions of both models are closer to the ground truth data in comparison to the other clusters, with the LSTM model closer to the ground truth data in more periods than the GRU models. It is important to notice that Cluster 10 is situated at the outskirt of the metropolitan area of Milan while Clusters 11 and 12 are closer to the center of the city.

The periods where the predictions of the DL models (for all clusters) are more distant from the ground truth data are in the Christmas period (24-26 December). During this period, the predictions of both models are much lower than the ground truth data. This can be explained easily by the seasonal, although predictable, traffic at that time. This could be addressed by augmenting the overall DL scheme with historical statistics that summarize prior knowledge of predictable long-term trends as per [37].

Based on our statistical tests, the LSTM models outperform the GRU models in all but one cluster. In that case, Cluster 12, the superior performance of the GRU model is relatively small. As shown in Figure 11, both RNNs capture the data pattern, however, the values predicted by the LSTM models are closer to the ground truth Internet activity data. This is not entirely surprising. As discussed in Section 2.2.2, typically LSTM is expected to outperform its less complex variant, GRU. We attribute the lower performance of the GRU to the lower complexity of the GRU units in comparison to the LSTM. Figure 11 shows that the predictions of the GRU model follow a similar pattern as the LSTM, but with lower values. These lower values increase prediction error, resulting in a higher RMSE and MAE. Notwithstanding this, the GRU model took less time to train, and thus, where a model needs to be retrained for multi-step traffic prediction, the benefits of efficiency gains (e.g. faster decision making, and computational and economic cost savings) may outweigh the differences in accuracy.

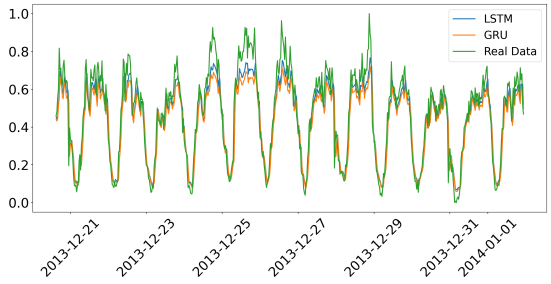


**(a)** Cluster 1

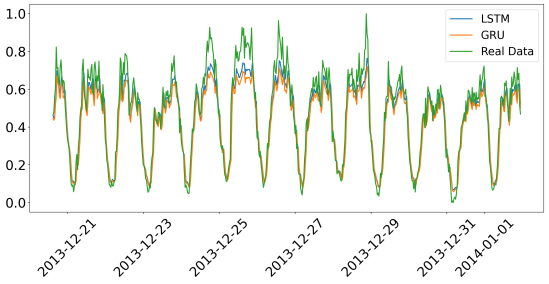


**(b)** Cluster 2

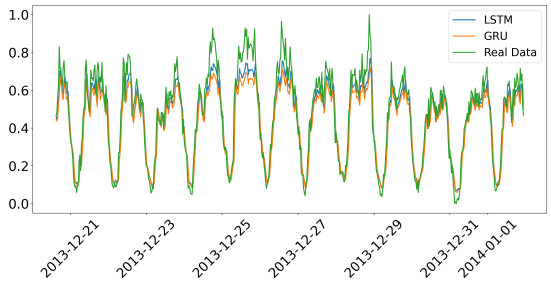


**(c)** Cluster 3

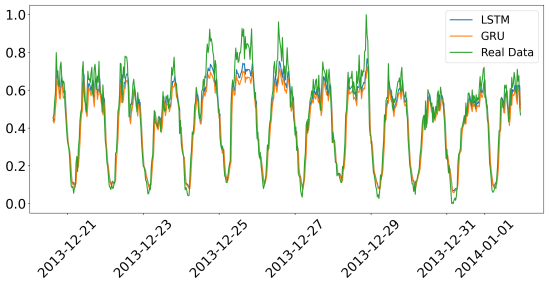


**(d)** Cluster 4

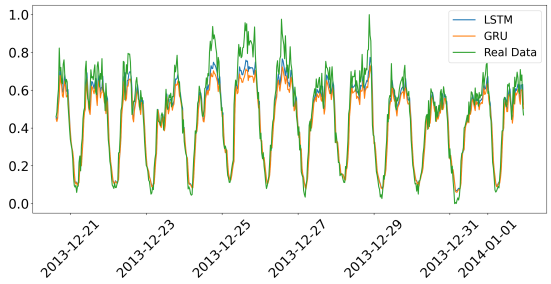


**(e)** Cluster 5

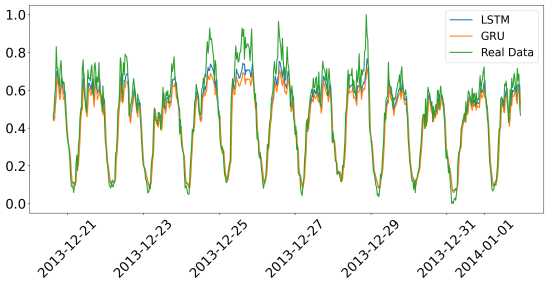


**(f)** Cluster 6

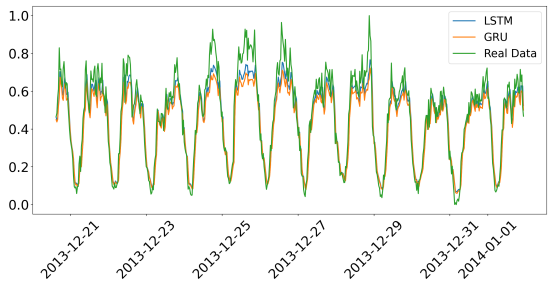


**(g)** Cluster 7

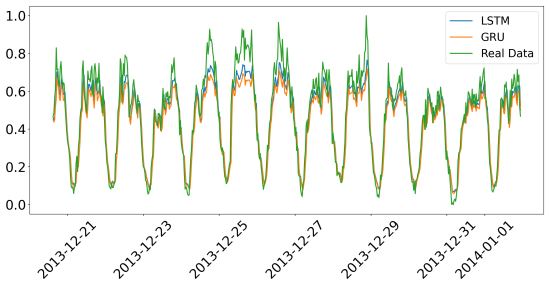


**(h)** Cluster 8

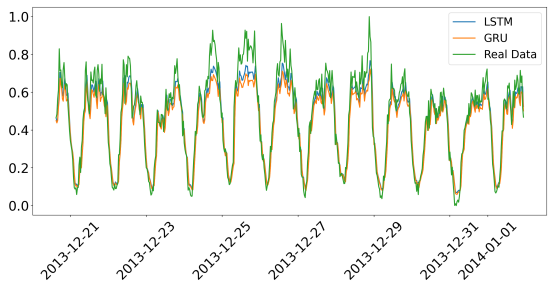


**(i)** Cluster 9

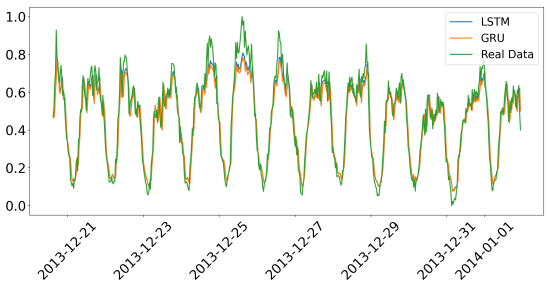


**(j)** Cluster 10

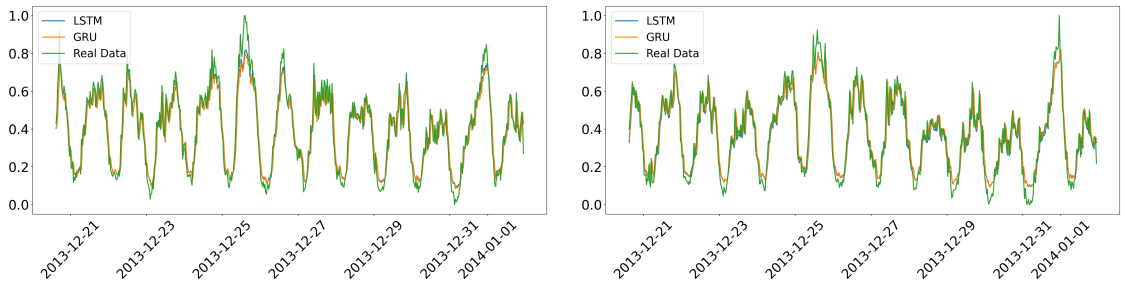


**(k)** Cluster 11 **(l)** Cluster 12

**Figure 11** Comparison of ground truth Internet activity and LSTM and GRU internet traffic predictions.

As discussed earlier, Chen et al. [16] also used the Telecom Italia dataset for Milan and an LSTM to predict base station traffic. While they used a clustering strategy at a group base stations level, it was *post hoc* i.e. they forecast the traffic patterns using the LSTM and *then* cluster complementary base stations to BBUs based on the traffic patterns. As such, the results presented by Chen et al. [16] are not entirely comparable with this study since they considered a different clustering strategy and a different time interval in their experiments. In fact, the different clustering approaches may result in different traffic patterns resulting in a direct impact on the model performance. Finding related works for direct comparison in the context of traffic prediction is a complex task as different studies may vary dataset, evaluation metrics, transformations, and data preprocessing. Notwithstanding the differences, Chen et al. [16] is the closest to study identified to that presented in this article, and consequently we use it as a basis for comparison. All average MAE values obtained for LSTM models were lower than the best result presented in [16], which was 0.074. For the GRU models, Cluster 1 obtained the same MAE as Chen et al. [16] (0.0739) while the models for the other clusters performed better. Cluster 12 achieved the best MAE. The LSTM presented an improvement of 26.22% and the GRU model presented an improvement of 27.16% when compared to the reported results in Chen et al. [16].

## 6 | CONCLUSION

Global total mobile data traffic is projected to grow 4X to reach 160EB per month in 2025; 5G networks will carry nearly half of the world's mobile data traffic by that time [57]. This massive surge in demand for mobile broadband requires solutions that satisfy QoS and QoE requirements with minimum service delay and within budget constraints. Mobile network traffic prediction will be an essential input into infrastructure planning as well as dynamic and proactive network resource optimization. Extant approaches may have unacceptable accuracy, training times, turnaround times, lack computational complexity and may not therefore account for characteristics such as bursting, non-linear patterns or other important correlations to meet the QoS and QoE requirements of increasingly demanding end users [6, 9]. These issues can result in mis-timed resource allocation as well as over- and under-utilization. DL has the potential to address these shortcomings.

In this work, we proposed and compared the performance of two RNNs, LSTM and GRU, to predict mobile Internet traffic in a large metropolitan area, Milan. We proposed a novel *a priori* clustering methodology to group cells using K-Means clustering and used the Grid Search method to identify the best configurations for each RNN. We compared RNN performance using RMSE and MAE, and testing against ground truth data for Milan. Both RNNs were effective in modeling Internet activity and seasonality, both within days and across two months however were sub-optimal in predicting anomalies e.g. Christmas. In this case, this could have been addressed by augmenting the training with historic trend data as per [37]. We also find variations by in clusters across the city. While the LSTM outperformed the GRU, the GRU had faster training times which may be relevant for multi-step prediction scenarios. We compared our results with Random Forest and Decision Tree, common ML model techniques used for time series prediction. Both LSTM and GRU models outperformed the ML models for all clusters of cells. We also compared our proposed RNN models against the results in Chen [16] using MAE. Notwithstanding the validity issues in such a comparison, results suggest our models present significantly better performance.

In future work, we plan to compare additional machine learning and deep learning architectures including ensemble approaches and augmenting the model with longer-term historical trend data. Furthermore, we will extend the dataset with more

heterogeneous data sources including SMS and voice call log data, amongst others, as well as other areas, e.g. Trentino, available in the Telecom Italia dataset. Improved mobile network prediction can be applied to a wide range of network planning and optimization use cases to optimise utilization, reduce cost and meet QoS. In future works, we will explore the efficacy of these models in a variety of use cases particularly where the faster training times of GRUs may provide advantages over LSTM, such as multi-step prediction and faster optimization time scales.

## ACKNOWLEDGEMENTS

The authors would like to thank the Fundação de Amparo a Ciência e Tecnologia de Pernambuco (FACEPE) for funding this work through grant IBPG-0059-1.03/19 and the Irish Institute of Digital Business (IIDB) at Dublin City University.

## References

1. GSMA . The Mobile Economy 2020. https://bit.ly/359YSAW; 2020. Accessed: April, 2020.

2. Cisco . Cisco Annual Internet Report. https://www.cisco.com/c/en/us/solutions/executive-perspectives/annual-internet-report/index.html; 2020. Accessed: April, 2020.

3. Aguzzi S, Bradshaw D, Canning M, et al. Definition of a research and innovation policy leveraging cloud computing and IoT combination. *Final Report, European Commission, SMART* 2013; 37: 2013.

4. Tikunov D, Nishimura T. Traffic prediction for mobile network using Holt-Winter's exponential smoothing. In: IEEE. ; 2007: 1–5.

5. Ma B, Guo W, Zhang J. A Survey of Online Data-Driven Proactive 5G Network Optimisation Using Machine Learning. *IEEE Access* 2020; 8: 35606–35637.

6. Narejo S, Pasero EGA. An Application of Internet Traffic Prediction with Deep Neural Network. 2018; 55: 139–149.

7. Bui N, Cesana M, Hosseini SA, Liao Q, Malanchini I, Widmer J. A survey of anticipatory mobile networking: Context-based classification, prediction methodologies, and optimization techniques. *IEEE Communications Surveys & Tutorials* 2017; 19(3): 1790–1821.

8. Li R, Zhao Z, Zheng J, Mei C, Cai Y, Zhang H. The learning and prediction of application-level traffic data in cellular networks. *IEEE Transactions on Wireless Communications* 2017; 16(6): 3899–3912.

9. Tran QT, Hao L, Trinh QK. Cellular network traffic prediction using exponential smoothing methods. *Journal of Information and Communication Technology* 2019; 18(1): 1–18.

10. Huang CW, Chiang CT, Li Q. A study of deep learning networks on mobile traffic forecasting. In: IEEE. ; 2017: 1–6.

11. Samulevicius S, Pedersen TB, Sorensen TB. MOST: Mobile Broadband Network Optimization Using Planned Spatio-Temporal Events. In: ; 2015: 1–5.

12. Pollakis E, Stanczak S. Anticipatory Networking for Energy Savings in 5G Systems.. *WSA* 2016: 1–7.

13. Hua Y, Zhao Z, Liu Z, Chen X, Li R, Zhang H. Traffic Prediction Based on Random Connectivity in Deep Learning with Long Short-Term Memory. In: ; 2018: 8690851.

14. Qiu C, Zhang Y, Feng Z, Zhang P, Cui S. Spatio-Temporal Wireless Traffic Prediction With Recurrent Neural Network. *IEEE Wireless Communications Letters* 2018; 7(4): 554–557.

15. Syarif I, Prugel-Bennett A, Wills G. SVM parameter optimization using grid search and genetic algorithm to improve classification performance. *Telkomnika* 2016; 14(4): 1502.

16. Chen L, Yang D, Zhang D, Wang C, Li J, Nguyen TMT. Deep mobile traffic forecast and complementary base station clustering for C-RAN optimization. *Journal of Network and Computer Applications* 2018; 121: 59–69.

17. Zhang C, Patras P, Haddadi H. Deep Learning in Mobile and Wireless Networking: A Survey. *IEEE Communications Surveys and Tutorials* 2019; 21(3): 2224–2287.

18. Kraus M, Feuerriegel S, Oztekin A. Deep learning in business analytics and operations research: Models, applications and managerial implications. *European Journal of Operational Research* 2020; 281(3): 628–641.

19. Guidotti R, Monreale A, Ruggieri S, Turini F, Giannotti F, Pedreschi D. A Survey Of Methods For Explaining Black Box Models. *ACM Computing Surveys* 2019; 51(5): 1–42.

20. Ansari M, Alsamhi S, Qiao Y, Ye Y, Lee B. Security of Distributed Intelligence in Edge Computing: Threats and Countermeasures. In: Theo Lynn PE, Lee B., eds. *The Cloud-to-Thing Continuum - Opportunities and Challenges in Cloud, Fog and Edge Computing*Cham, Switzerland: Palgrave Macmillan. 2020.

21. Ordóñez FJ, Roggen D. Deep convolutional and lstm recurrent neural networks for multimodal wearable activity recognition. *Sensors* 2016; 16(1): 115.

22. Hochreiter S. The vanishing gradient problem during learning recurrent neural nets and problem solutions. *International Journal of Uncertainty, Fuzziness and Knowledge-Based Systems* 1998; 6(02): 107–116.

23. Jozefowicz R, Zaremba W, Sutskever I. An empirical exploration of recurrent network architectures. In: ; 2015: 2342–2350.

24. Greff K, Srivastava RK, Koutník J, Steunebrink BR, Schmidhuber J. LSTM: A search space odyssey. *IEEE transactions on neural networks and learning systems* 2017; 28(10): 2222–2232.

25. Yan S. Understanding LSTM and its diagrams. https://bit.ly/2JvRwhr; 2016. Accessed: August, 2018.

26. Lin HY, Hsueh YL, Lie WN. Abnormal Event Detection Using Microsoft Kinect in a Smart Home. In: IEEE. ; 2016: 285–289.

27. Chung J, Gulcehre C, Cho K, Bengio Y. Empirical evaluation of gated recurrent neural networks on sequence modeling. *arXiv preprint arXiv:1412.3555* 2014.

28. Chung J, Gulcehre C, Cho K, Bengio Y. Gated feedback recurrent neural networks. In: ; 2015: 2067–2075.

29. Kaiser Sutskever I. Neural GPUs Learn Algorithms. *arXiv preprint arXiv:1511.08228* 2015.

30. Arkhipenko K, Kozlov I, Trofimovich J, Skorniakov K, Gomzin A, Turdakov D. Comparison of neural network architectures for sentiment analysis of Russian tweets. *Computational Linguistics and Intellectual Technologies. International Conference*.

31. Na S, Xumin L, Yong G. Research on k-means clustering algorithm: An improved k-means clustering algorithm. In: Ieee. ; 2010: 63–67.

32. Rai P, Singh S. A survey of clustering techniques. *International Journal of Computer Applications* 2010; 7(12): 1–5.

33. Arora P, Varshney S, others . Analysis of k-means and k-medoids algorithm for big data. *Procedia Computer Science* 2016; 78: 507–512.

34. Zhang C, Zhang H, Yuan D, Zhang M. Citywide cellular traffic prediction based on densely connected convolutional neural networks. *IEEE Communications Letters* 2018; 22(8): 1656–1659.

35. Wang J, Tang J, Xu Z, et al. Spatiotemporal modeling and prediction in cellular networks: A big data enabled deep learning approach. In: ; 2017: 1–9.

36. Alawe I, Ksentini A, Hadjadj-Aoul Y, Bertin P. Improving Traffic Forecasting for 5G Core Network Scalability: A Machine Learning Approach. *IEEE Network* 2018; 32(6): 42–49.

37. Zhang C, Patras P. Long-Term Mobile Traffic Forecasting Using Deep Spatio-Temporal Neural Networks. In: ; 2018: 231–240.

38. Feng J, Chen X, Gao R, Zeng M, Li Y. DeepTP: An End-to-End Neural Network for Mobile Cellular Traffic Prediction. *IEEE Network* 2018; 32(6): 108–115.

39. Eurostat . Population on 1 January by age groups and sex - cities and greater cities. 2020.

40. Barlacchi G, De Nadai M, Larcher R, et al. A multi-source dataset of urban life in the city of Milan and the Province of Trentino. *Scientific data* 2015; 2: 150055.

41. Hussain B, Du Q, Zhang S, Imran A, Imran MA. Mobile Edge Computing-Based Data-Driven Deep Learning Framework for Anomaly Detection. *IEEE Access* 2019; 7: 137656–137667.

42. Mededovic E, Douros VG, Mähönen P. Node Centrality Metrics for Hotspots Analysis in Telecom Big Data. In: IEEE. ; 2019: 417–422.

43. Zhang D, Liu L, Xie C, Yang B, Liu Q. Citywide Cellular Traffic Prediction Based on a Hybrid Spatiotemporal Network. *Algorithms* 2020; 13(1): 20.

44. Amin F, Choi GS. Hotspots Analysis Using Cyber-Physical-Social System for a Smart City. *IEEE Access* 2020; 8: 122197–122209.

45. Yuan C, Yang H. Research on K-value selection method of K-means clustering algorithm. *J—Multidisciplinary Scientific Journal* 2019; 2(2): 226–235.

46. Syakur M, Khotimah B, Rochman E, Satoto B. Integration K-means clustering method and elbow method for identification of the best customer profile cluster. In: . 336. IOP Publishing. ; 2018: 012017.

47. Kingma DP, Ba J. Adam: A method for stochastic optimization. *arXiv preprint arXiv:1412.6980* 2014.

48. Wang W, Lu Y. Analysis of the mean absolute error (MAE) and the root mean square error (RMSE) in assessing rounding model. In: . 324. IOP Publishing. ; 2018: 012049.

49. Zeng Q, Sun Q, Chen G, Duan H, Li C, Song G. Traffic Prediction of Wireless Cellular Networks Based on Deep Transfer Learning and Cross-Domain Data. *IEEE Access* 2020; 8: 172387–172397.

50. Kuber T, Seskar I, Mandayam N. Traffic prediction by augmenting cellular data with non-cellular attributes. In: IEEE. ; 2021: 1–6.

51. Shen W, Zhang H, Guo S, Zhang C. Time-Wise Attention Aided Convolutional Neural Network for Data-Driven Cellular Traffic Prediction. *IEEE Wireless Communications Letters* 2021.

52. Chai T, Draxler RR. Root mean square error (RMSE) or mean absolute error (MAE)?–Arguments against avoiding RMSE in the literature. *Geoscientific model development* 2014; 7(3): 1247–1250.

53. Zang Y, Ni F, Feng Z, Cui S, Ding Z. Wavelet transform processing for cellular traffic prediction in machine learning networks. In: IEEE. ; 2015: 458–462.

54. Troia S, Alvizu R, Zhou Y, Maier G, Pattavina A. Deep learning-based traffic prediction for network optimization. In: IEEE. ; 2018: 1–4.

55. Cao S, Liu W. Lstm network based traffic flow prediction for cellular networks. In: Springer. ; 2019: 643–653.

56. Elliott AC, Hynan LS. A SAS® macro implementation of a multiple comparison post hoc test for a Kruskal–Wallis analysis. *Computer methods and programs in biomedicine* 2011; 102(1): 75–80.

57. Ericsson . Ericsson Mobility Report: 5G uptake even faster than expected. https://mb.cision.com/Main/15448/2836925/1060118.pdf; 2019. Accessed: April, 2020.

**How to cite this article:** Williams K., B. Hoskins, R. Lee, G. Masato, and T. Woollings (2016), A regime analysis of Atlantic winter jet variability applied to evaluate HadGEM3-GC2, *Q.J.R. Meteorol. Soc.*, *2017;00:1–6*.